Journal of the European Ceramic Society **17** (1997) 259–266
© 1996 Elsevier Science Limited
Printed in Great Britain. All rights reserved
PII: S0955-2219(96)00130-6
0955-2219/97/$17.00

Influence of pH on the Pressure Slip Casting of Silicon Carbide Bodies

J. M. F. Ferreira & H. M. M. Diz

Department of Ceramics and Glass Engineering/INESC, University of Aveiro, 3800 Aveiro, Portugal

(Received 15 September 1995; revised version received 12 September 1996; accepted 15 September 1996)

Abstract

The effect of interparticle forces and applied pressure on the kinetics of the pressure slip casting process, on cake compressibility, and on the green properties of the resulting silicon carbide bodies was investigated. The structure of particle aggregates in the suspensions was determined by electrophoretic measurements, particle size analysis, and rheological techniques. The relative green density, water content and pore size distributions of the consolidated bodies were measured and a good correlation found between the properties of the pressure cast bodies and the structure of the initial suspensions. © 1996 Elsevier Science Limited.

1 Introduction

The forming of ceramics can be accomplished by several different techniques. Colloidal processing of ceramic powders results in more homogeneous packing of the particles in comparison with consolidation technology based on dry pressing.[1] Slip and pressure slip casting are also suitable techniques to produce bodies with complex shapes. However, the limited suction capacity of plaster moulds makes slip casting occur slowly even when steps to maximize the deposition rate are followed.[2] This limitation is particularly noticed when well dispersed slurries and/or particle size distributions that allow the formation of high packing density structures are used.[3] Unlike slip casting, pressure casting derives its main driving force from an external pressure applied to the ceramic suspension which results in an increased rate of cake formation.[4] Other advantages of pressure casting are reviewed elsewhere.[3]

The kinetics of pressure casting obeys Darcy's differential equation[5] for fluid flow through porous media, which, when integrated with appropriate boundary conditions, shows that the thickness of the consolidated layer, L, formed when either pressure, P, or time, t, is kept constant, is parabolically related to the variation in the other of these experimental variables by the equation

$$L^2 = 2K\phi\, Pt/\eta(\phi_c - \phi) \quad (1)$$

where η is the liquid viscosity and ϕ and ϕ_c are the volume fractions of particles within the slurry and cake, respectively. The permeability, K, is inversely related to the resistance to fluid flow through the consolidated layer. This equation assumes unidirectional filtration, negligible mould resistance, constant rheological properties of the suspension, absence of particle settling, and constant permeability, i.e. the body is incompressible.

In practice, cakes are more or less compressible, depending on pressure level,[6] interaction forces between particles,[7–9] and particle size distributions.[3] As a result, some moisture and/or density gradient and, hence, permeability gradient would be expected, causing deviations from linearity in the relations L^2 versus P or L^2 versus t. Some authors[6] have suggested that permeability is a function of the effective pressure expressed as

$$K = K_0 P^{-s} \quad (2)$$

where s is the coefficient of compressibility. If $s = 0$, the cake is incompressible ($K = K_0$); if $s = 1$, the body is totally compressible. Combining eqns (1) and (2), the body formation rate (wall thickness squared and divided by the elapsed time) can be represented by

$$L^2/t = 2K_0 P^{1-s}\phi/\eta(\phi_c - \phi) \quad (3)$$

The influence of pH on the rheological behaviour, suspension stability and slip casting performance of the silicon carbide powders used in this work has already been studied.[10] The aim of the present

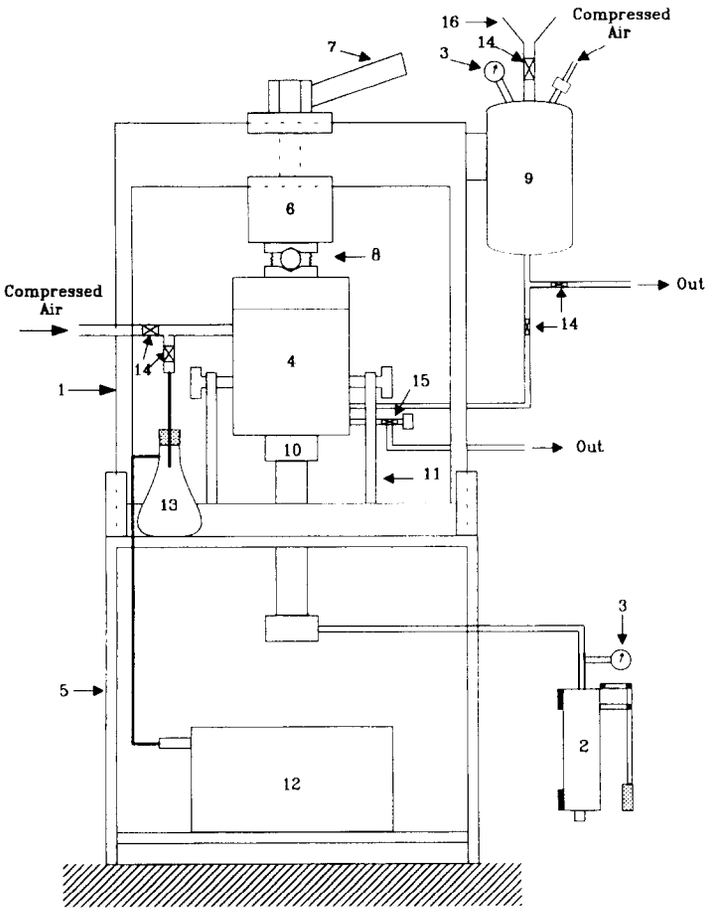

Fig. 1. Schematic of pressure slip casting machine: (1) press 15 ton; (2) hydraulic unit; (3) manometers; (4) pressure chamber; (5) metallic support; (6) fixed paten; (7) threaded clamp; (8) spherical alignment jig; (9) slip holding tank; (10) piston; (11) lateral guides; (12) vacuum pump; (13) Erlenmeyer flask; (14) sphere valves; (15) needle valve; (16) funnel.

work was to evaluate the influence of slurry structure, as controlled by pH, on the kinetics of pressure slip casting and to relate this with the microstructure of the formed bodies.

2 Experimental Procedure

2.1 Materials and reagents

The starting material was a silicon carbide powder, NF0, supplied by Elektroschmelzwerk, Kempten, GmBH, Germany, with a mean diameter of 1·2 μm. Solutions of hydrochloric acid and sodium hydroxide were used to adjust the pH values of suspensions. A solution of sodium chloride was used to adjust the ionic strength in electrophoretic and floc size experiments. All reagents were p.a. grade (Merck Portuguesa, Lda., Portugal).

2.2 Techniques

The suspension preparation procedure[10] can be summarized as follows. The powders were first added to distilled water with hand stirring, followed by ultrasonication for 10 min. The pH was then adjusted to the required values and ultrasonication allowed for another 10 min. The solid content of the suspensions was limited to 62·5 wt% because of their high viscosity at and near the isoelectric point.

The pressure slip casting experiments were performed in a laboratory pressure casting unit built for this purpose which is schematically shown in Fig. 1. The press was inverted on a metallic support and fitted with a fixed paten which could slide horizontally to allow the pressure chamber to be opened or closed. The pressure chamber was connected with the slip holding tank through a closed circuit to allow the admission of compressed air or its evacuation with a vacuum pump. The filling and emptying operations could be done in a few seconds. The system could be connected to the waste network and thoroughly rinsed with water. Figure 2 shows a detail of the pressure chamber and the mould mounting system. The moulds were hollow cylinders with outer and inner diameters of 0·07 m and 0·008 m, respectively, and 0·025 m height, encapsulated in stainless steel.

The system was first evacuated for 15 min. The rubber tubes connecting the slip holding tank with the pressure chamber were then filled under vacuum. After that, compressed air was admitted in

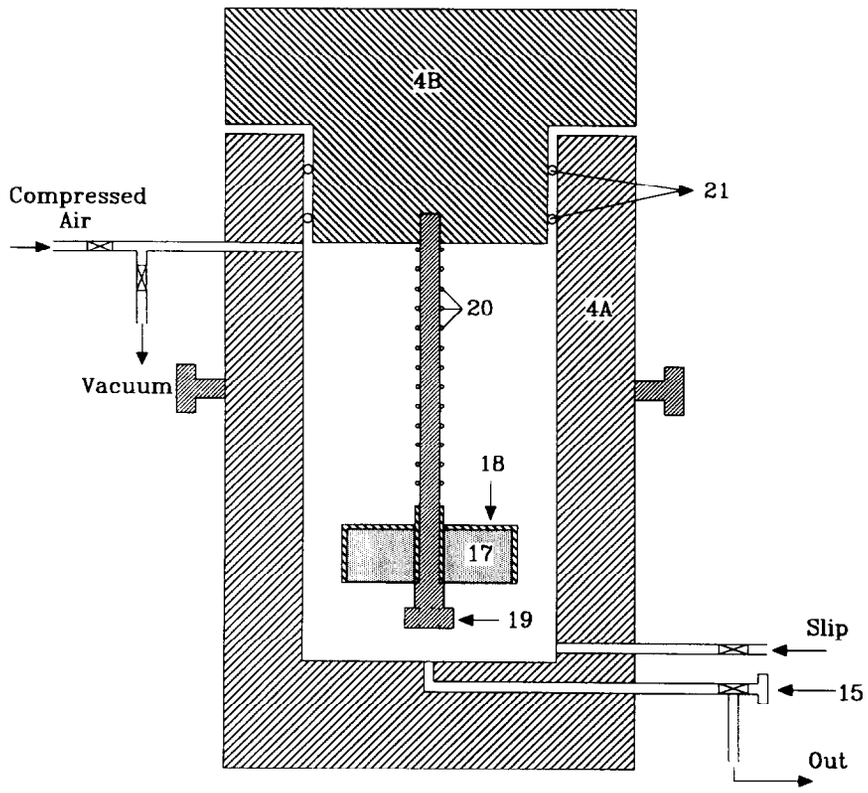

Fig. 2. Schematic of pressure chamber: (4A) pressure chamber body; (4B) pressure chamber lid; (17) plaster mould; (18) stainless steel capsule; (19) supporting screw; (20) helicoidal spring; (21) O-rings.

the slip holding tank and the pressure chamber brought to pressure. The level of pressure was maintained with compressed air if the applied pressure was ≤588 kPa, or with the hydraulic unit for higher pressures.

The pore size and pore size distributions of the green bodies were determined with a porosimeter PoreSizer 9320 (Micromeritics). The high-pressure part of each experiment was run in the automatic mode with an equilibration time of 10 s at each point.

3 Results and Discussion

3.1 Slurry characterization

The results of the electrophoretic mobility, floc size distributions, Bingham yield stress and plastic viscosity, already reported,[10] can be summarized as follows. The isoelectric point was located at pH ≈ 2 where the floc size was larger, the floc size distributions broader, and the Bingham yield stress and plastic viscosity exhibited maximum values. At the isoelectric point, electrical double layer repulsions are absent and the van der Waals attractions dominate. As a consequence, aggregates are readily formed when particles collide due to Brownian movements; these grow heavy and sink. The variation of pH away from the isoelectric point, results in the development of charge on the surface of the particles and repulsive double layer forces between them, reducing their collision efficiency, according to the DLVO theory of colloid stability.[11,12] Consequently, the floc size decreased as well as the Bingham yield stress and plastic viscosity. The finest and narrowest floc size distributions was observed at pH 8, where the zeta potential was maximum; the particle size distribution was assumed to be that of the powder. Lower values for the rheological parameters were also observed at about pH 8.

3.2 Pressure casting

The effects of applied pressure and pH on the green density and wall thickness for a given time are presented in Figs 3 and 4, respectively. It can be seen that the density is practically independent

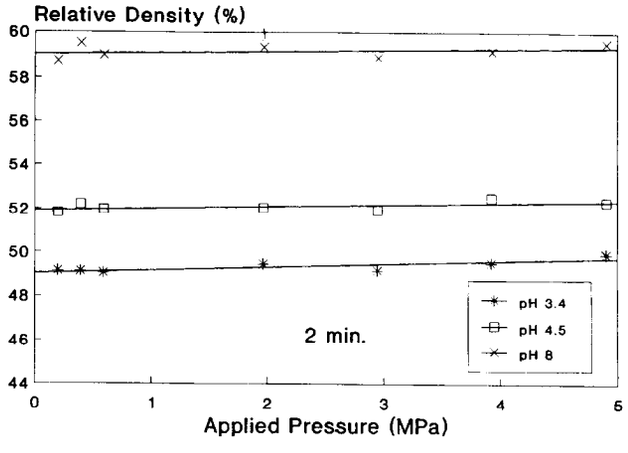

Fig. 3. Effect of applied pressure and pH on green density.

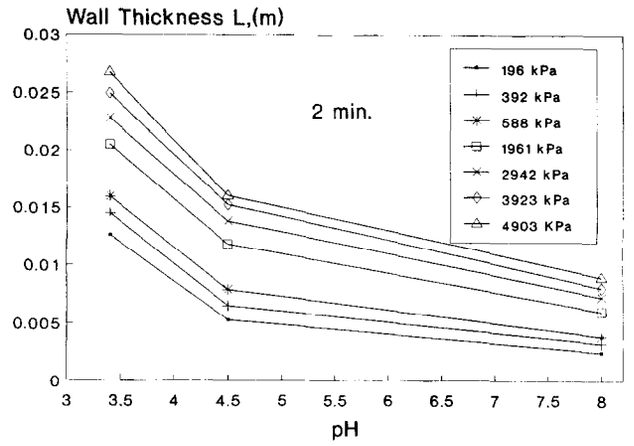

Fig. 4. Effect of pH and applied pressure on wall thickness, L.

of pressure for the dispersed slurry (pH 8), and only slightly dependent for the less stable slurries, while wall thickness strongly depends on both variables. The effects of the same experimental variables on mean pore size distributions are shown in Fig. 5. The higher green densities are observed at pH 8 where the electrophoretic mobility showed a maximum[10] and interactions between particles are dominated by the electrostatic repulsive forces. This close relationship between interparticle forces, rheological properties of the suspensions and the properties of the green bodies indicates that the structure of particles in suspension is transmitted to the solid wall being formed near the surface of the mould, as already suggested.[13] These results are consistent with observations made by Fennelly and Reed[7,8] and Lange and Miller[9] who found that dispersed slurries produce much higher packing densities relative to flocced slurries. In addition, Lange and Miller found that the packing density of the dispersed slurries was relatively pressure-insensitive, whereas the packing density of the flocced slurries was very pressure-sensitive. This last point differs from the present observations.

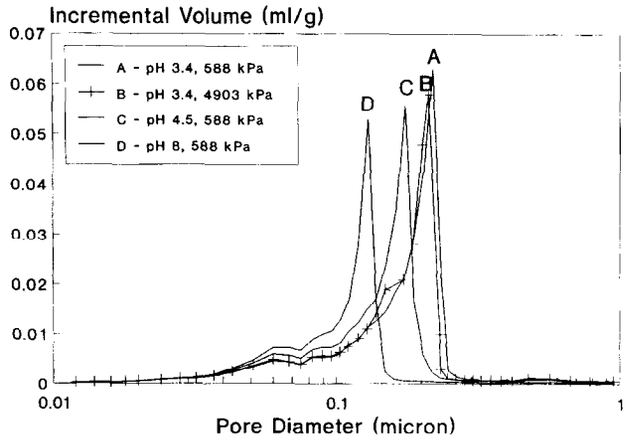

Fig. 5. Effect of pH and applied pressure on mean pore size distributions.

The repulsive interparticle forces within the dispersed slurry allow the particles to flow and pack as individuals. Since particles are still repulsive as they join the consolidation layer, they are free, within certain translational limits, to move to positions of lowest free energy. This 'spontaneous' particle rearrangement should be a determining factor for the high packing densities obtained in normal casting in plaster moulds.[10,14] When pressure is added to the suction pressure of the mould the number of particles that reach the interface between cake and slurry, per unit time, increases. The spontaneous lateral movements of one particle can now be restricted by new incoming particles. So, less extensive spontaneous rearrangement and a decrease in packing density should be expected.

On the other hand, as the pH varies towards the isoelectric point of the surface particles, they attract each other, due to van der Waals attraction forces, and form low-density clusters.[15] When such clusters are added to the consolidation layer they form a more open and permeable network structure, which is expected to be less stable with regard to applied pressure.[1,16] Figure 5 confirms that at pH 3·4 the increase in applied pressure from 588 kPa to 4903 kPa results in pore narrowing, while at pH 8 the pore size distribution curves are practically coincident. As discussed by Kuhn *et al.*[17] a touching particle network can be in static equilibrium with regard to an applied consolidation pressure. At an incrementally higher pressure, this network becomes unstable when the force on any particle which can fill a vacant position exceeds a critical value. This instability leads to particle rearrangement, the formation of a new network in static equilibrium with the applied pressure, and an increase in packing density. Thus, for a given particle size distribution, the maximum packing density depends on 'spontaneous' and 'forced' particle rearrangements. The first contribution is favoured by strong repulsive interparticle forces and low values for the slip casting driving force (the suction pressure of the mould plus applied pressure), whereas, the second is favoured by attractive interparticle forces and by the use of high values for the applied pressure. So, the applied pressure has contradictory effects on particle packing density.

Because of the high deposition rate at pH 3·4, the mould becomes rapidly saturated, and casting times longer than 2 min cannot be used. The effects of applied pressure and casting time on green density and cake thickness were accordingly studied at pH 4·5 and 8. Figure 6 shows that the green density increases with increasing casting time in what appears to be a parabolic dependency. The curves tend to superimpose, illustrating

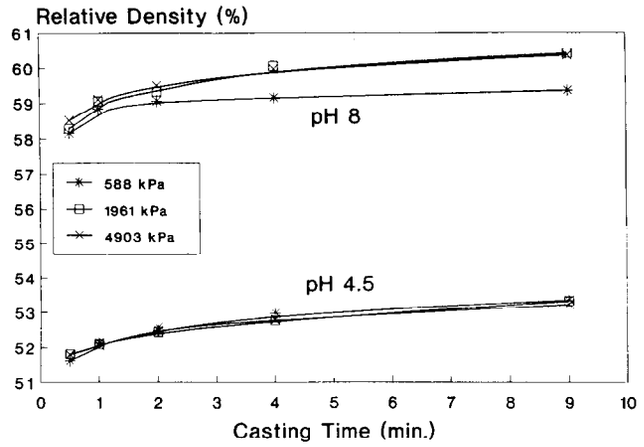

Fig. 6. Effect of casting time and applied pressure on green packing density.

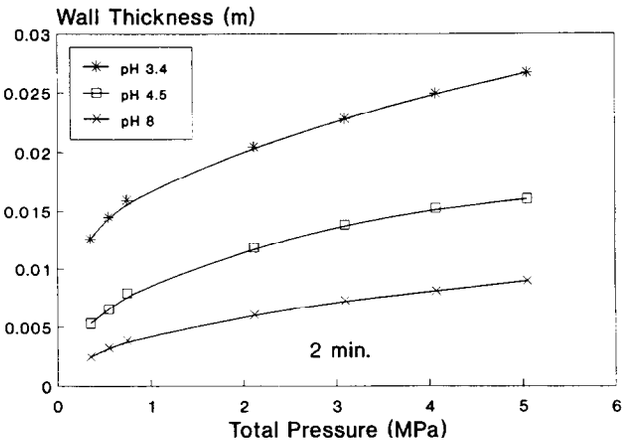

Fig. 8. Evolution of wall thickness as a function of total pressure.

again the limited influence of pressure on green density and the small extent of 'forced' particle rearrangements. The differences observed at 588 kPa and pH 8 were unexpected because these conditions are the most favourable to 'spontaneous' particle rearrangements. However, the maximum measured differences were only about 1% of the theoretical density and can be due to unforseen causes such as entrapment of air bubbles in the consolidated layer or even experimental error. The results are consistent with the decrease in pore volume and the narrowing of pore diameters observed in Fig. 7, and seem to be mainly due to an increase in 'spontaneous' particle rearrangement permitted by the slowing of deposition rates with elapsed time. The same arguments could be used to interpret results obtained by other authors.[6,9,18,19] Frassek and Hennicke[6] used computer tomography to determine the density profiles of cast bodies and noticed that in unilateral casting, the density on the side away from the mould was significantly higher. A more pronounced secondary shrinkage on that side was admitted to account for the observed difference. However, this explanation

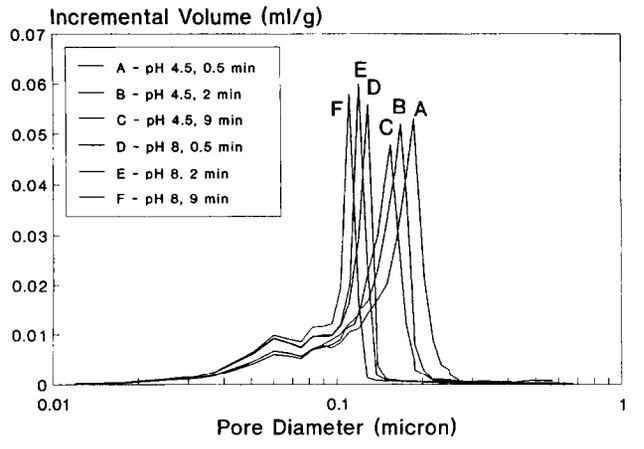

Fig. 7. Effect of pH and casting time on mean pore size distributions.

seems hardly convincing. In effect no differential shrinkage or consequent body damage was reported by the authors, and both should happen if their suggestions were correct. Lange and Miller[9] measured alumina cake permeability as a function of applied pressure. A slight increase and a considerable decrease, for dispersed and flocced slurries, respectively, was observed. Novich and Pyatt[18] used very well-dispersed alumina slurries to study the effect of filtration rate on the properties of green and sintered bodies and found a systematic increase in both green and sintered porosity with increasing filtration rates. High filtration rates also resulted in less uniform microstructures. Kotte *et al.*[19] reported an increase in cake porosity with applied pressure for a deflocculated silicon nitride system. This increase in cake porosity was attributed to the slightly dilatant behaviour of the suspension, caused by a high solids content. But it is worthy of note that a high solids content is not favourable to 'spontaneous' particle rearrangements.

The evolution of wall thickness as a function of total pressure, P_t, (suction pressure of the mould + applied pressure), shown in Fig. 8 seems to obey the parabolic law, eqns (1) or (3). To decide which equation best fits our data, we plot log L^2 versus log P_t in Fig. 9, which also indicates the slope of the straight lines represented. It can be seen that the slopes differ from unity. This difference (the coefficient of compressibility, s) decreases with an increase in suspension stability and at pH 8 the structure formed is almost incompressible. These results are in good agreement with observations made by Fennelly and Reed[7,8] and Lange and Miller.[9]

Our data are best described by eqn (3), which can be rewritten in the form

$$L^2 = AKP_t^{1-s}(t_0+t) \qquad (4)$$

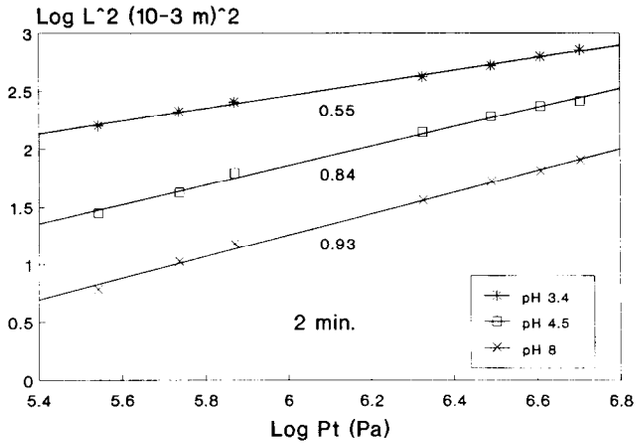

Fig. 9. Evidence for the cake compressibility.

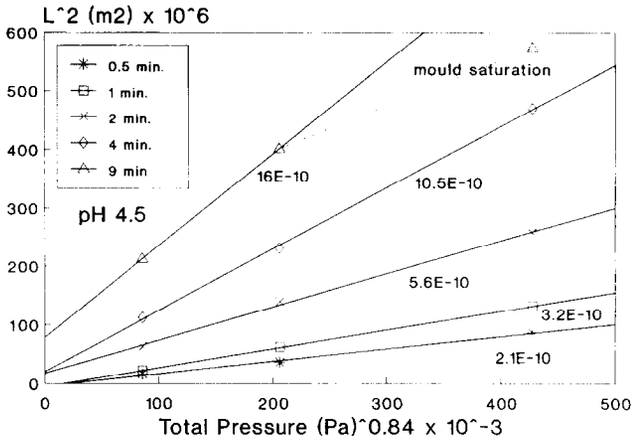

Fig. 11. Effect of total pressure and casting time on wall thickness at pH 4·5.

where t_0, is the set-up time (the time required to fill the pressure chamber and to adjust the pressure level, which was usually about 0·1 min), and the parameter A is given by

$$A = 2\phi/\eta(\phi_c - \phi) \tag{5}$$

Plots of L^2 against P_t^{1-s} are shown in Figs 10–12, together with the slopes of the straight lines represented. The cake permeabilities can be calculated from the slopes indicated, assuming $t_0 = 0{\cdot}1$ min and that A remains constant during the casting process. The results are presented in Table 1 and enable the following conclusions to be drawn: (1) the pressure has only a minor influence on cake permeability, which seems to decrease slightly with the increments in this variable; (2) permeability is very sensitive with regard to the casting time, especially at pH 4·5, which is consistent with the increase in green density observed in Fig. 6, and with the pore narrowing shown in Fig. 7.

Figure 11 shows that for higher casting time and pressure the cake thickness does not follow the initial trend, because of the mould saturation effect. Figures 11 and 12 also show that the straight lines deviate from the origin of the axis to an extent that increases with casting time and when less stable (pH 4·5) suspensions are used. These deviations cannot be attributed to the mould resistance because its permeability is three to four orders of magnitude higher than the cake permeabilities formed at pH 4·5.[3] They can be explained in terms of a set-up time effect and variations in cake permeability with casting time. Both contribute to lowering the slope of the straight lines represented, as will be demonstrated.

3.2.1 Effect of set-up time

By defining a new parameter

$$B = A.K_p.P_t^{1-s} \tag{6}$$

eqn (4) can be rewritten in the following simplified form

$$L^2 = B(t_0 + t) = Bt_0 + Bt \tag{7}$$

with the body formation rate being described by

$$L^2/t = B(t_0/t + 1) \tag{8}$$

This function predicts a decrease in the slope of the straight lines shown in Figs 11 and 12 with increasing casting times. Figure 13 represents that

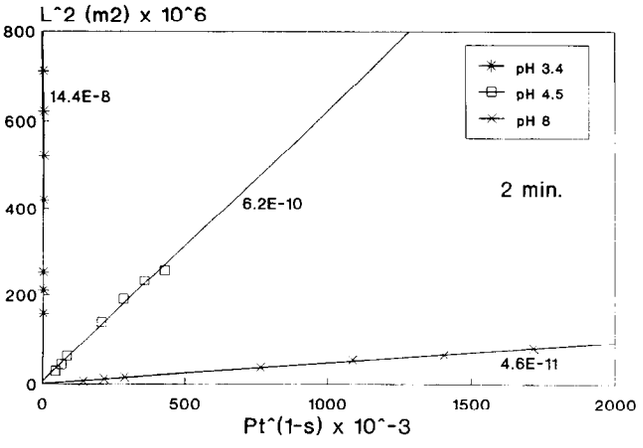

Fig. 10. Effect of total pressure and pH on wall thickness.

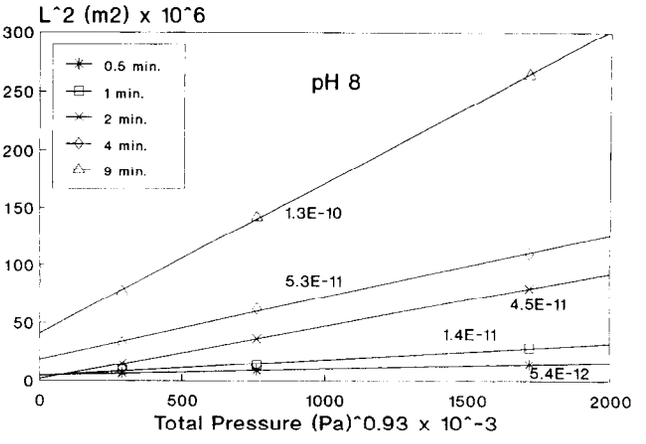

Fig. 12. Effect of total pressure and casting time on wall thickness at pH 8.

Table 1. Effect of casting time and applied pressure on cake permeabilities

Experimental variable		*Permeability, K (m^2) × 10^{15}*	
		pH 4·5	*pH 8*
Casting time (min)	0·5	90	2·3
	1	67	3·0
	2	60	4·8
	4	56	2·8
	9	38	3·1
Applied pressure (kPa)	588	58	5·9
	1961	44	4·5
	4903	56	3·6

function for t_0 = 0·1 min at three different values of $P_l^{(1-s)}$ (1 MPa, 5 MPa and 10 MPa), as well as its absolute cumulative variations confirming the effect.

3.2.2 Effect of cake permeability variations

From the increase in green density (Fig. 6) and pore narrowing (Fig. 7), a gradual decrease in cake permeability with casting time is expected. The A parameter defined by eqn (5) decreases and, as a consequence, the body formation rate decreases faster than predicted by eqn (4). Assuming that the green density evolution obeys a parabolic law, as suggested in Fig. 6, the solid volume fraction in the cake as a function of time can be written as

$$\phi_p = \phi_{p0} + \Delta\phi(t) \quad (9)$$

The function $\Delta\phi(t)$ determined from the green density variations at pH 4·5, using the average of three measurements, is

$$\Delta\phi(t) = -0{\cdot}00142 + 0{\cdot}0058\sqrt{t} \quad (10)$$

After neglecting the small and time-independent constant, this function is shown in Fig. 14 for the same three pressure values used in Section 3.2.1.

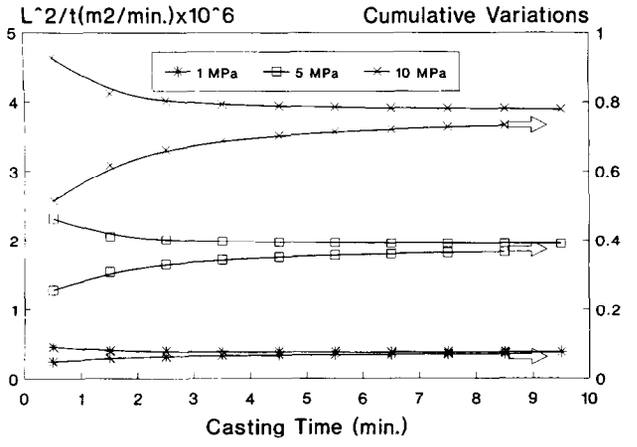

Fig. 13. Evidence for the effect of set-up time on body formation rate.

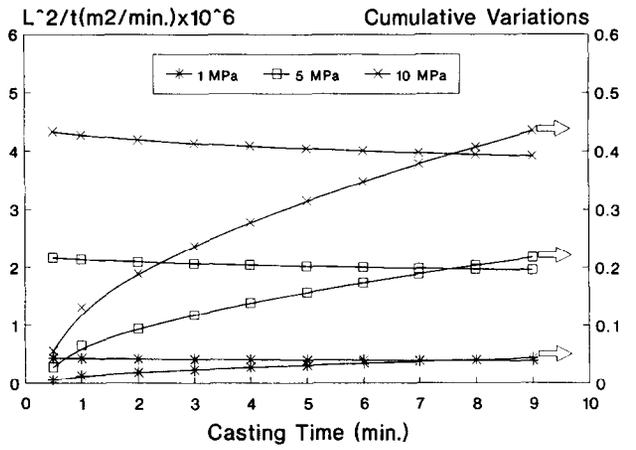

Fig. 14. Evidence for the effect of changes in cake permeability on body formation rate.

To separate the influence of set-up time, t_0 = 0 was used. This result confirms the contribution of cake permeability variations to lowering the slope of the straight lines represented in Figs 11 and 12.

4 Conclusions

1. Interparticle potentials play a dominant role in governing the body formation rate, green packing density, compressibility and microstructure of the formed green bodies.
2. To achieve high packing densities, strong repulsive interparticle potentials are required, which can be controlled by suspension pH.
3. Cake permeability and green density are virtually insensitive to the applied pressure and slightly dependent on casting time. This last effect as well as the set-up time effect contribute to a decrease in body formation rate.

References

1. Lange, F. F., Powder processing science and technology for increased reliability. *J. Am. Ceram. Soc.*, **72** (1989) 3.
2. Tiller, F. M. & Hsyung, N. B., *J. Am. Ceram. Soc.*, **74** (1991) 210.
3. Ferreira, J. M. F., A. Interface carboneto de silício-solução aquosa e o enchimento por barbotina. PhD Thesis, Departamento de Engenharia Cerâmica e do Vidro, Universidade de Aveiro, 1992.
4. Blanchard, E. G., Pressure casting improves productivity, *J. Am. Ceram. Bull.*, **67** (1988) 1680.
5. Tiller, F. M. & Tsai, C. D., Theory of filtration of ceramics: I, Slip casting. *J. Am. Ceram. Soc.*, **69** (1986) 882.
6. Frassek, L. & Hennicke, H. W., Some aspects of pressure slip casting with nonclay suspensions. *Ceram. Forum Intern.*, **67** (1990) 443.
7. Fennelly, T. J. & Reed, J. S., Mechanics of pressure slip casting. *J. Am Ceram. Soc.*, **55** (1972) 264.
8. Fennelly, T. J. & Reed, J. S., Compression permeability of Al_2O_3. *J. Am. Ceram. Soc.*, **55** (1972) 381.

9. Lange, F. F. & Miller, K. T., Pressure filtration: Consolidation kinetics and mechanics. *Am Ceram. Soc. Bull.*, **66** (1987) 1498.
10. Ferreira, J. M. F. & Diz, H. M. M., Effect of slurry structure on the slip casting of silicon carbide powders. *J. Europ. Ceram Soc.*, **10** (1992) 59.
11. Derjaguin, B. V. & Landau, L. D., Theory of stability of highly charged lyophobic sols and adhesion of highly charged particles in solutions of electrolytes. *Acta Physico-Chim. URSS*, **14** (1941) 633.
12. Verwey, J. W. & Overbeek, J. Th. G., *Theory of Stability of Lyophobic Colloids*. Elsevier Science Publishers, Amsterdam, 1948.
13. Diz, H. M. M. & Ferreira, J. M. F., Study of the factors influencing the slip casting of mullite–zirconia ceramics. *Brit. Ceram. Proc. of Special Ceramics* **8**, ed. S. P. Howlett, & D. Taylor, 1986, p. 159.
14. Ferreira, J. M. F. & Diz, H. M. M., Effect of the amount of Deflocculant and powder size distribution on the green properties of silicon carbide bodies obtained by slip casting. *J. Hard Materials*, **3** (1992) 17.
15. Firth, B., Flow properties of coagulated colloidal suspensions. II. Experimental properties of the flow curve parameters. *J. Coll. Interf. Sci.*, **57** (1976) 257.
16. Velamakanni, B. V. & Lange, F. F., Effect of interparticle potentials and sedimentation on particle packing density of bimodal particle size distributions during pressure filtration. *J. Am. Ceram. Soc.*, **74** (1991) 166.
17. Kuhn, L. K, McMecking, R. M. & Lange, F. F., A model for powder consolidation. *J. Am. Ceram. Soc.*, **74** (1991) 682.
18. Novich, B. E. & Pyatt, D. H., Consolidation behavior of high performance ceramic suspensions. *J. Am. Ceram. Soc.*, **73** (1990) 207.
19. Kotte, J. F. A. K, Denissen, J. A. M. & Metselaar, R. Pressure casting of silicon nitride, *J. Europ. Ceram. Soc.*, **7** (1991) 307–314.